DTM GENERATION FROM SPOT HRS IN-TRACK STEREO IMAGES

Th. Toutin [a, *], P. Briand[b], R. Chénier[c]

[a] Natural Resources Canada, Canada Centre for Remote Sensing, 588 Booth St., Ottawa, Ontario, K1A 0Y7 Canada - thierry.toutin@ccrs.nrcan.gc.ca
[b] Canadian Space Agency, 6767 route de l'Aéroport, St-Hubert, Quebec, J3Y 8Y9 Canada - paul.briand@space.gc.ca
[c] Consultants TGIS inc., 16 chemin Pelletier, Chelsea, Quebec, J9B 2A6 Canada - rene.chenier@ccrs.nrcan.gc.ca

KEY WORDS: Photogrammetry, DEM/DTM, SPOT-5, Stereoscopic, Accuracy

ABSTRACT:

A preliminary version of the 3D multi-sensor physical model developed at the Canada Centre for Remote Sensing was developed for the generation of digital elevation models (DEM) from SPOT-5 HRS in-track stereo images (pixel of 5 m by 10 m). Even if three accurate ground control points (GCPs) were enough to set-up the stereo bundle adjustment, ten stereo GCPs collected from 1:20,000 map were used and the 3D modeling was checked on independent points: errors of 14 m, 9 m and 4.7 m in *X*, *Y* et *Z* were obtained. Since these errors included the feature extraction error, the internal accuracy of the stereo modeling is better than a pixel. The DEM was then generated using an area-based multi-scale image matching method and 3D semi-automatic editing tools and then compared to LIDAR elevation data with to 0.2-m accuracy. Errors of 5.5 m and 10 m with confidence levels of 68% (LE68) of 90% (LE90), respectively is achieved over the full LIDAR area. Since the DEM is in fact a digital surface model where the height of land covers is included, accuracies were computed over the bare surfaces only: LE68 of 2.7 m and LE90 of 5.6 m with no bias were achieved. In addition, the same process was applied to SPOT-5 HRG across-track stereo images (5 m pixel) and equivalent results were obtained: LE68 of 6.5 m and LE90 of 10 m with 2 m bias over the full LIDAR area, and LE68 of 2.2 m and LE90 of 5 m with -2 m bias over the bare surfaces. However, relatively to the stereo-acquisition geometry, the results with HRG ("1/3 pixel") were better than the results with HRS ("1/2 pixel"). Equivalent results (stereo modelling and elevation extraction) should be thus obtained for HRS data with the final version of the 3D physical model.

RÉSUMÉ :

Une version préliminaire du modèle physique 3D du Centre canadien de télédétection a été développée pour la création de modèles numériques d'altitude (MNA) à partir de couple stéréoscopique d'images HRS avant-arrière de SPOT-5 (pixel de 5 m par 10 m). Même si que trois points d'appui précis (PAs) sont nécessaires pour calculer la compensation des gerbes stéréo, dix PAs stéréo acquis à partir de cartes au 1 : 20000 et la modélisation a été vérifiée avec des points indépendants : des erreurs de 14 m, 9 m et 4,7 m en *X*, *Y* et *Z* ont été obtenues. Comme ces erreurs incluent l'erreur d'extraction cartographique, la précision interne de la modélisation stéréo est meilleure que le pixel. Le MNA a été alors créé avec une méthode de corrélation de surface d'images multi-échelle et des outils d'édition semi-automatique, puis comparé à des données LIDAR d'une précision de 0,20 m. On a obtenu des erreurs de 5,5 m et de 10 m avec des niveaux de confiance de 68% (LE68) et de 90% (LE90), respectivement pour toute la surface du LIDAR. Mais comme le MNA est en fait un modèle numérique de surface, qui inclut la hauteur de la couverture du sol, on a alors calculé les précisions sur les surfaces nues seulement : des LE68 de 2,7 m et LE90 de 5,6 m sans biais sont alors obtenues. De plus, le même procédé a été appliqué à des images stéréoscopiques HRG droite-gauche (pixel de 5 m) et on a obtenu des résultats équivalents : LE68 de 6,5 m et LE90 de 10 m avec un biais de 2 m pour la surface totale du LIDAR, et LE68 de 2,2 m et LE90 de 5 m avec un biais de -2 m pour la les surfaces nues. Par contre en tenant compte de la géométrie d'acquisition stéréoscopique, les résultats avec HRG (« 1/3 pixel ») sont meilleurs que ceux avec HRS (« 1/2 pixel »). Des résultats équivalents (modélisation stéréo et extraction d'altitude) seront alors obtenus pour les données HRS avec la version finale du modèle physique 3D.

1. INTRODUCTION

To obtain stereoscopy with images from satellite scanners, two solutions are possible: (1) the along-track stereoscopy from the same orbit using fore and aft images, and (2) the across-track stereoscopy from two different orbits (Toutin, 2001).

The latter solution was more used since 1980: firstly, with Landsat from two adjacent orbits (Ehlers and Welch, 1987), then with SPOT-1 (Denis, 1986) to SPOT-5 (Bouillon *et al.*, 2002) using across-track steering capabilities, and finally with IRS-1C/D by "rolling" the satellite (Gopala Krishna, 1996). In the last few years the first solution as applied to space frame cameras got renewed popularity with the JERS-1's Optical Sensor (Raggam and Almer, 1996), the German Modular Opto-Electronic Multi-Spectral Stereo Scanner (Ackermann *et al.*, 1995), the Advanced Spaceborne Thermal Emission and Reflection Radiometer (Welch *et al.*, 1998; Toutin, 2002) and the French SPOT-5 High-Resolution-Stereoscopy (HRS) (Bouillon *et al.*, 2002).

The objectives of this study are to evaluate the capabilities of the SPOT-5 HRS same-date in-track sensor to generate digital elevation models (DEMs) and to compare with its multi-date along-track HRG sensor. The 3D multi-sensor physical model

* Corresponding author.

developed at Canada Centre for Remote Sensing (CCRS) for medium-resolution sensors in the visible and infra-red (MODIS, MERIS, Landsat, SPOT, ASTER, etc.) as well as in the microwave (SIR-C, JERS, ERS-1, RADARSAT, ENVISAT) (Toutin, 1995), was adapted these last years for high resolution data, such as SPOT-5 HRG across-track data (Toutin, 2004). A preliminary version has been recently developed for SPOT-5 HRS in-track stereo-data and is used in this study.

2. STUDY SITE AND DATA SET

2.1 Study Site

The study site is an area north of Québec City, Québec, Canada (47º N, 71º 30' W). This study is an urban, rural and forested environment and has a hilly topography in the south with a mean slope of 7º, and mountainous topography in the north with a mean slope of 10º and maximum slopes of 30º. The elevation ranges from 0 m at the St-Lawrence River to 1000-m in the Canadian Shield. Québec City is in the south-east part.

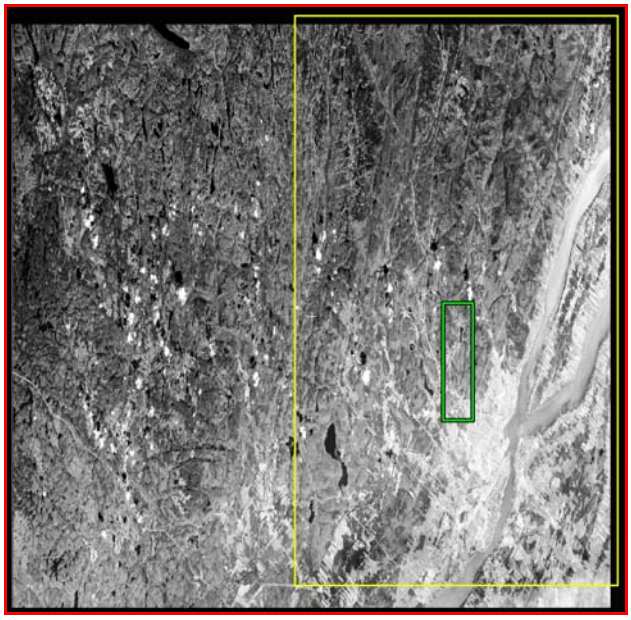

Figure 1. SPOT-5 HRS fore image, acquired north of Québec City, Canada (120 km by 60 km; 10 m by 5 m pixel spacing). The yellow box represents the across-track stereo-pair (60 km by 60 km) and the green box the Lidar (5 km by 13 km).
SPOT-5 © 2003 CNES and Courtesy SPOT-IMAGE

2.2 Data Set

The ±22° in-track stereo-images (120 km by 60 km; 10 m by 5 m pixel spacing; base-to-height ratio, *B/H*, of 0.85) were acquired September 18, 2003 as a courtesy of SPOT-Image, France with 5% of clouds and their shadows (Figure 1). The SPOT-5 images are raw level-1A data, orbit oriented, with detector equalization only. Ephemeris and attitude data are available in the metadata as well as general information related to the sensors and satellite.

In addition, SPOT-5 HRG across-track stereo-pair (Figure 1 yellow box; 60 km by 60 km; 5 m by 5 m pixel spacing; *B/H* of 0.77) was acquired on May 5 and 25, 2003 with viewing angles of +23º and -19º, respectively. The May 5 image displays snow in the forests (upper part) and frozen lakes (lower left and centre), for almost 50% of the image, but not the May 25 image. These differences in snow/ice generated large radiometric differences in SPOT stereo-images. However, these differences provide an opportunity to test DEM generation method and address potential problems in difficult conditions instead of working in a perfect environment.

To evaluate the accuracy of the stereo-extracted DEMs, accurate spot elevation data was obtained from a LIDAR survey conducted by GPR Consultants (www.lasermap.com) on September 6th, 2001 (Figure 1 green box). The Optech ALTM-1020 system is comprised of a high frequency optical laser coupled with a Global Positioning System and an Inertial Navigation System. The ground point density is about 300,000 3-D points per minute and the accuracy is 0.30 m in planimetry and 0.15 m in elevation. Since it was impossible to cover the full SPOT stereo-pair (60 km by 120 km), ten swaths covering an area of 5 km by 13 km (Fig. 1) and representative of the full study site were acquired. The results of the LIDAR survey are then an irregular-spacing grid (around 3 m), due also to no echo return in some conditions such as buildings with black roofs, roads and lakes. Since the objectives of this research study were to evaluate the stereo DEMs, the LIDAR elevation data was not interpolated into a regular spacing grid so as to avoid the propagation of interpolation error into the checked elevation and evaluation.

3. EXPERIMENT

Since the processing steps of DEM generation using either in-track or across-track stereo images are well known, the six processing steps are summarized in Figure 2 (Toutin, 1995):

1. Acquisition and pre-processing of the remote sensing data (images and metadata) to determine an approximate value for each parameter of 3D physical model for the two images;
2. Collection of stereo GCPs with their 3D cartographic coordinates and two-dimensional (2D) image coordinates. GCPs covered the total surface with points at the lowest and highest elevation to avoid extrapolations, both in planimetry and elevation. Ninety-eight and thirty-three GCPs were acquired for in- and across-track stereo-pairs, respectively from 1:20,000 topographic maps (2-3 m accuracy in the three axes). The image pointing accuracy was less than one pixel.
3. Computation of the stereo models, initialized with the approximate parameter values and refined by an iterative least-squares bundle adjustment (coplanarity equations) with the GCPs (Step 2) and orbital constraints. Both equations of colinearity and coplanarity are used as observation equations and weighted as a function of input errors. Theoretically three accurate GCPs are enough to compute the stereo model, but more GCPs were acquired either to have an overestimation in the adjustment and to reduce the impact of errors or to perform accuracy tests with independent check points (ICPs).
4. Extraction of elevation parallaxes using multi-scale mean normalized cross-correlation method with computation of the maximum of the correlation coefficient. This method gave good results and was commonly used with satellite VIR images (Gülch, 1991);
5. Computation of *XYZ* cartographic coordinates from elevation parallaxes (Step 4) using the previously-

computed stereo-model (Step 3) with 3D least-squares stereo-intersection; and

6. Generation of regular grid spacing with 3D automatic and 3D visual editing tools: automatic for blunders removal and for filling the small mismatched areas and visual for filling the large mismatched areas and for the lakes.

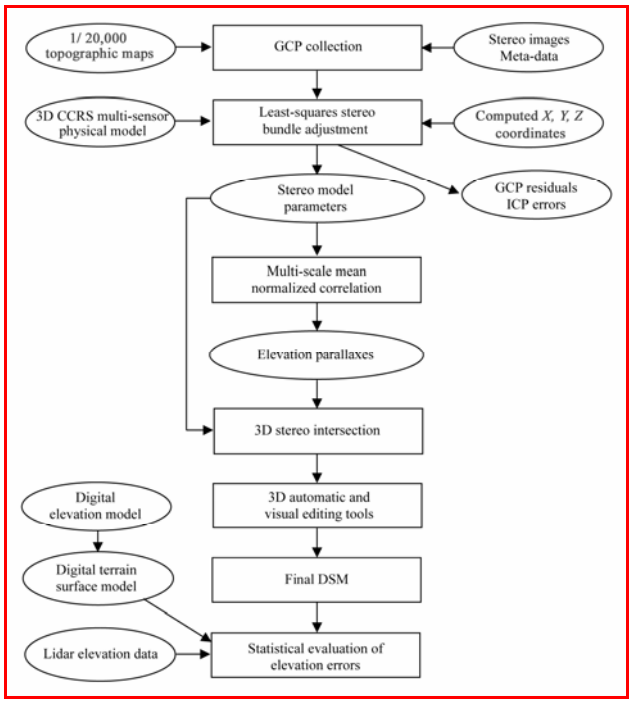

Figure 2. Processing steps for the generation of DEMs from stereo-images and their evaluation with LIDAR data.

The DEM is then evaluated with the lidar elevation data. About 5 300 000 points corresponding to the overlap area were used in the statistical computation of the elevation accuracy. Different parameters (land cover and its surface height), which have an impact on the elevation accuracy, were also evaluated.

4. RESULTS

4.1 Results on The Stereo-Model Computations

As a function of the number of GCPs used in the stereo bundle adjustments, two sets of tests were performed for each stereo-pair. Set 1 was conducted with all the GCPs while Set 2 was performed with a reduced number of GCPs (10-18) and the remaining points as ICPs. In Set 2, 10 GCPs were used because previous results demonstrated that this was a good compromise with this dataset to avoid the propagation of input data error (cartographic and image pointing) into the 3-D physical stereo-models (Toutin, 2004).

Test Stereo	GCP/ ICP	GCP RMS Residuals (m)			ICP RMS Errors (m)		
		X	*Y*	*Z*	*X*	*Y*	*Z*
1-HRS	98/0	10.1	7.6	3.8	-	-	-
1-HRG	33/0	2.6	3.1	3.3	-	-	-
2-HRS	**10**/88	7.1	6.4	3.1	**13.9**	**8.7**	**4.7**
2-HRG	**10**/23	1.5	1.4	1.3	**2.6**	**2.2**	**2.9**

Table 1. Results from the least-square bundle adjustment of the 3D physical model for the stereo-pairs (HRS in-track and HRG across-track): with the number of GCPs and ICPs, *XYZ* RMS residuals and errors (in metres) on GCPs and ICPs, respectively.

Table 1 gives for each stereo-pair the number of GCPs and ICPs, the root mean square (RMS) residuals and errors (in metres) of the least-square adjustment computation for the GCPs and ICPs, respectively. GCP RMS residuals reflect modelling and GCP accuracy, while ICP RMS errors reflect restitution accuracy, which includes feature extraction error and thus are a good estimation of the geopositioning accuracy of planimetric features. However, the final internal accuracy of the 3D modeling will be better than these RMS errors.

Due to the large redundancy of equations in the adjustments of Set 1, the RMS *X*-*Y* residuals are on the same order of magnitude as the input data errors, being a combination of image pointing error (one pixel) and planimetric error (3 m) in addition to the propagation of *Z*-error (3 m) depending on the viewing angles. With HRS stereo-pair, the differential pointing error due to a rectangular pixel is well reflected in all RMS results On the other hand, the RMS *Z* residuals (3.8 m and 3.3 m) approximately reflect GCP image pointing error (3 to 5 m) with *B/H* of 0.85 and 0.77 for the HRS and HRG stereo-pairs, respectively. The use of overabundant GCPs in the least-squares adjustment reduced or even cancelled the propagation of the input data errors into the 3-D physical stereo-models, but conversely these input errors are reflected in the residuals. Consequently, it is “normal and safe” to obtain RMS residuals from the least squares adjustment in the same order of magnitude as the input data error; however, the modelling or internal accuracy is better (less than one pixel).

Set 2 of the tests enabled unbiased validation of the 3D positioning and restitution accuracies with independent check data. First, the RMS residuals on GCPs are 20-40% smaller than the RMS residuals resulting from Set 1 because fewer GCPs, and thus less equation redundancy, were used in the least-squares adjustments. On the other hand, RMS errors on ICPs are 9-14 m and 2-3 m or when compared to sensor resolution, one-and-half and half-pixel for in- and across-track stereo-pairs, respectively. The worse results with in-track stereo-pair are due to the preliminary version of the 3D physical model for HRS data. Equivalent results with the final version of the 3D physical model for HRS data should be thus obtained for the stereo modelling (half-pixel).

Finally, the *Z*-RMS errors on ICPs are a good indication of the potential accuracy for the DEMs. However, these RMS errors, which include the extraction error (image pointing error of half-pixel) of ICP features, are only an estimation of the 3-D restitution accuracy of planimetric and elevation features, but the internal accuracy of stereo-models is thus better, in the order of sub-pixel.

4.2 Results on DEM Evaluations

The second result is the qualitative and visual evaluation of the full DEMs and the quantitative and the statistical evaluation of the DEMs with the LIDAR data. Figure 3 is the full DEM (120 km by 60 km; 10 m by 5 m grid spacing) in the image reference extracted from the in-track stereo-pair and Figure 4 is a sub-area (5 km by 5 km; 5-m grid spacing) over the LIDAR area but in the map reference. The black areas (5% of the total area) correspond to mismatched areas due to clouds and their shadows, as well as the lakes and the St. Lawrence River. The black dots in Figure 4 are the blunders, which were

automatically removed but not interpolated. The full DEM well reproduces the terrain relief and the different cartographic and topographic features, which can be seen in Figure 1: such as the mountains and valleys, the Saint-Lawrence River and its large island. Even small relief features between the mountains and the Saint-Lawrence River valley were captured. Much more topographic details are more noticeable in Figure 4.

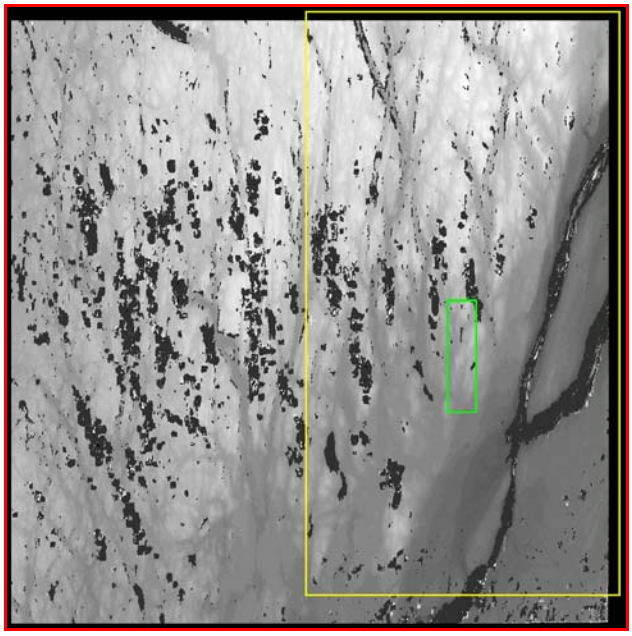

Figure 3. DEMs extracted from in-track HRS stereo-images (120 km by 60 km; 10 m by 5 m grid spacing). The black areas are the 5% mismatched areas. The yellow box represents the HRG DEM (60 km by 60 km) and the green box the Lidar (5 km by 13 km). SPOT-5 2003 Courtesy SPOT-IMAGE

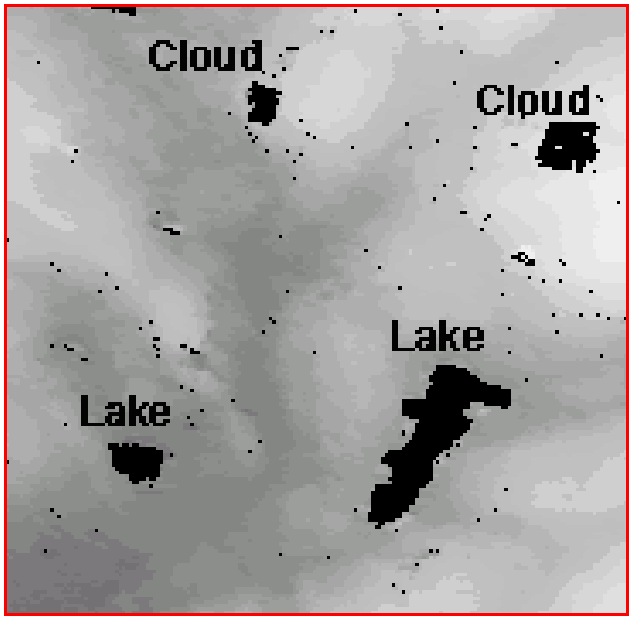

Figure 4. Sub-area (5 km by 5 km; 5 m grid spacing) of DEM extracted from HRS stereo-images. The large black areas are the mismatched areas and the small black dots are the blunders, removed but not interpolated. SPOT-5 2003 Courtesy SPOT-IMAGE

Quantitative evaluation of DEMs was conducted with the comparison of the LIDAR elevation data in the overlap area and five to six million elevation points were used in statistical computations. Table 2 gives the results computed from elevation errors for the HRS and HRG DEMs: the linear errors with 68% and 90% levels of confidence (LE68 and LE90, respectively), the bias and the percentage of class over three times LE68 (in metres).

DEM	Area Evaluation	LE68 (m)	LE90 (m)	Bias (m)	Over Three LE68
HRS	Total surface	5.5 m	10 m	2 m	2.2%
HRG	Total surface	6.5 m	10 m	2 m	0.7%
HRS	Bare surfaces	**2.7 m**	**5.6 m**	0.2 m	4%
HRG	Bare surfaces	**2.2 m**	**5.0 m**	-2 m	3%

Table 2. Statistical evaluation of DEMs stereo-extracted from HRS in-track and HRG across-track stereo-pairs for the total area and the bare surfaces: linear errors with confidence levels of 68% (LE68) and 90% (LE90), bias, and percentage over three LE68.

For HRS DEM, LE68 of 5.5 m was achieved and are good compared to the stereo bundle adjustment RMS *Z*-errors on well-defined ICPs (4.7 m). LE68 corresponds to an image matching error a little less than ±1 pixel (line spacing of 5 m and *B/H* of 0.85), which is similar to previous results generally achieved with different VIR medium-resolution stereo-images (1-pixel image matching accuracy) (Gülch, 1991). While LE68 (6.5 m) of HRG DEM is a little worse than HRS LE68 due to its smaller *B/H*, the same image matching error of ±1 pixel (pixel spacing of 5 m and *B/H* of 0.77) is obtained.

The largest errors (three times LE68), although representing only a very small percentage, are out of tolerance and cannot be acceptable for DEM in a topographic sense. In order to locate and understand these largest errors, they were superimposed on the DEMs or the ortho-images. Most of these large errors resulted from the elevation comparison of the top of tree versus the ground due to the different spatial resolutions of SPOT and LIDAR data and to the different acquisition seasons (deciduous with or without leaves). These errors are then specific of the cartographic data and study site largely covered by forests, but are not representative of the general SPOT stereo-performance for bald DEM generation. In fact, these DEMs stereo-extracted from HR data are digital surface models (DSMs), which include the height of natural and human-made surfaces. The smaller sensor resolution and the more accurate the DEM, the more noticeable are the height of some surfaces and the resulting cartographic features. Consequently, a second elevation accuracy evaluation was performed only on bare surfaces, where there is also no difference between the SPOT stereo-extracted elevation and the LIDAR data.

These results over bare surfaces (Table 2): LE68 of 2.7 m and 2.2 m for HRS and HRG DEMs, respectively are very good relatively to the pixel spacing. These results are also more consistent with *a priori* 3-D restitution accuracy computed from the stereo-bundle adjustments over ICPs (around 4.7 m and 2.9 m in *Z*, respectively). The largest percentage of errors over three LE68 (3-4%) is due to isolated trees in the bare surfaces. Strangely, the multi-date HRG acquisition (5 m pixel spacing and *B/H* of 0.77) achieved a parallax error of one-third of pixel, better than the half-pixel error achieved with the same-date HRS acquisition (5 m line spacing and *B/H* of 0.85). It is

mainly due to the preliminary version of the 3D physical model for HRS data and better results will be thus obtained with the final version. These last results obtained over bare surfaces better indicate the real stereo-performance for elevation extraction and DEM generation with SPOT in- and across-track stereo-images. Finally, when compared to other high-resolution sensors (Toutin, 2004), better results, relatively to resolution were obtained with SPOT-5 in- and across-track stereo acquisitions; some of the reasons could be the use of raw data (original geometry and radiometry) and an higher altitude with fewer orbital perturbations.

5. CONCLUSIONS

DEMs were extracted from two different stereo acquisitions with SPOT-5 (*B/H* of 0.85 for in-track and of 0.77 for across-track) using the 3-D CCRS physical geometric model and a multi-scale image matching. The stereo bundle adjustments of geometric models using ten GCPs enabled *a priori* 3-D restitution accuracy, which includes feature extraction error, to be estimated: one-and-half and half-pixel for in- and across-track stereo-pairs, respectively. However, the internal accuracy of the stereo-models is about sub-pixel. The stereo-extracted DEMs were then compared to accurate elevation LIDAR data, and LE68 of 5.5 m and 6.5 m were obtained for in- and across-track stereo-pairs, respectively. Since the surface heights were included in terrain elevation and its evaluation, elevation errors were thus evaluated on bare surfaces, where there is no elevation difference between the stereo DEMs and the LIDAR data. The results over bare surfaces (2.7 m and -2.2 m LE68 for in- and across-track stereo-pairs, respectively) are a good indication of the general SPOT-5 stereo-performance for DEM generation. However, relatively to the stereo-acquisition geometry (*B/H*), the results with HRG ("1/3 pixel") were better than the results with HRS ("1/2 pixel"). Equivalent results with the final version of the 3D physical model for HRS data should be thus obtained for the stereo modelling (half-pixel) and for DEM over bare surfaces ("1/3 pixel").

ACKNOWLEDGEMENTS

The authors thank Mr. Marc Bernard and Didier Giacobbo from SPOT-Image for the two stereo-pairs, *GPR Consultants* (Québec, Canada) for the LIDAR survey and Mr. Réjean Matte du *Ministère des Ressources naturelles du Québec*, Canada for the cartographic data. They also thank Ms. Susann Nitzsche and Irene Walde of *Hochschule für Technik und Wirtschaft Dresden (FH)*, Germany for processing the data.

REFERENCES

Ackerman, F., D. Fritsch, M. Hahn, F. Schneider, V. Tsingas, 1995. Automatic generation of digital terrain models with MOMS-02/D2 data, *Proceedings of the MOMS-02 Symposium*, Köln, Germany, July 5-7, (Paris, France: EARSeL), pp. 79-86.

Bouillon, A., E. Breton, F. de Lussy, R. Gachet, 2002. SPOT5 HRG and HRS first in-flight geometric quality results, *Proc. of SPIE, Vol. 4881A Sensors, System, and Next Generation Satellites VII*, Agia Pelagia, Crete, Greece, 22-27 September, (Bellingham, WA: SPIE), CD-ROM (Paper 4881A-31).

Ehlers, M., R. Welch, 1987, "Stereo-correlation of Landsat-TM images", *Photogrammetric Engineering and Remote Sensing*, 53(9), pp. 1231-1237

Denis, P., 1986. Génération de modèle numérique de terrain à partir de données SPOT, *International Archives of Photogrammetry and Remote Sensing*, Rovamieni, Finland, August 19-22, (Helsinki, Finland: ISPRS), 26(B3/2), pp. 176-185.

Gopala Krishna, B., B. Kartikeyan, K.V. Iyer, Rebantrea Mitra, P.K. Srivastava, 1996. Digital photogrammetric workstation for topographic map updating using IRS-1C stereo imagery, *International Archives of Photogrammetry and Remote Sensing*, Vienna, Austria, July 9-18, (Vienna, Austria: Austrian Society for Surveying and Geoinformation), 31(B4), pp. 481-485.

Gülch, E., 1991. Results of Test on Image Matching of ISPRS WG III/4, *ISPRS Journal of Photogrammetry and Remote Sensing*, 46(1), pp. 1-8.

Raggam, J., A., Almer, 1996. Assessment of the potential of JERS-1 for relief mapping Using optical and SAR data, *International Archives of Photogrammetry and Remote Sensing*, Vienna, Austria, July 9-18, (Vienna, Austria: Austrian Society for Surveying and Geoinformation), 31(B4), pp. 671-676.

Toutin, Th., 2004. Comparison of Stereo-Extracted DTM from Different High-Resolution Sensors: SPOT-5, EROS, IKONOS and QuickBird, *IEEE-TGARS*, 42(9), (in press). http://dweb.ccrs.nrcan.gc.ca/ccrs/db/biblio/paper_e.cfm?BiblioID=13383 (accessed 9 May 2004).

Toutin Th., 2002. Three-Dimensional Topographic Mapping with ASTER Stereo Data in Rugged Topography, *IEEE-TGARS*, 40(10), pp. 2241-2247. http://www.ccrs.nrcan.gc.ca/ccrs/rd/sci_pub/bibpdf/13119.pdf (accessed 9 May 2004).

Toutin, Th., 2001. Elevation modelling from satellite visible and infrared (VIR) data: a review, *International Journal of Remote Sensing*, 22(6), pp. 1097-1225. http://www.ccrs.nrcan.gc.ca/ccrs/rd/sci_pub/bibpdf/13072.pdf (accessed 9 May 2004).

Toutin, Th., 1995. Generating DEM from Stereo-Images with a Photogrammetric Approach: Examples with VIR and SAR data, *EARSeL Advances in Remote Sensing*, 4(2), pp. 110-117. http://www.ccrs.nrcan.gc.ca/ccrs/rd/sci_pub/bibpdf/13150.pdf (accessed 9 May 2004).